from the x-polarization. As the incident polarization changes from y to x, the MTM changes rapidly from a negative index to a positive index material.

The cross-board MTM is inherently lossy, due to the forbidden band regions associated with single negative materials; the material exhibits negative permittivity for E_y incident polarization, and negative permeability for E_x incident polarization. A change in polarization is not observed in the cross-board MTM structure, due to the dynamic range limitations of the experiment.

5. CONCLUSION

The polarization properties of the 1D MTM lenses have been investigated and the results are compared with a 2D MTM lens. In the 2D MTM structure, the transmitted MW radiation was found to be elliptically polarized (for E_y), whereas no such change in polarization was noted for the 1D lens. A good agreement with experiment and modeling results was observed. The polarization response for a given SRR+R configuration is attributable to the coupling mechanisms of the MTM constituent elements to the incident MW radiation. As the incident polarization changes from y to x, the 1D lens transitions from a net negative index of refraction material to a positive index material. For the cross-board configuration, at resonance frequency, the MTM exhibits negligible transmission due to forbidden bands, attributable to either negative permittivity (for E_y) or negative permeability (for E_x). The cross-board MTM exhibits negative permittivity for an E_y polarized state and negative permeability for an E_x polarized state. The MW radiation transmitted through MTMs is significantly affected by the polarization state of the incident beam. As MTMs are deployed in applications it is necessary to account for their polarization response. Furthermore, the control of transmission through the polarization state of the incident radiation allows for the possibility of fabrication of novel MTM devices.

REFERENCES

1. D.A. McGillivray, R.L. Cravey, K.L. Dudley, E. Vedeler, and M.C. Gupta, Polarization properties of a 2-D split ring resonator and rod type metamaterial lens, IEEE Trans Antennas Propag. In press.
2. J.B. Pendry, Negative refraction makes a perfect lens, Phys Rev Lett 85 (2000), 3966–3969.
3. D. Shreiber, Ph.D. thesis, University of Virginia, 2008..
4. K. Aydin, M.Sc. thesis, Bilkent University, Turkey, 2004.
5. R.A. Shelby, D.R. Smith, and S. Schultz, Experimental verification of a negative index of refraction, Science 292 (2001), 77–79.
6. D.R. Smith, Design and measurement of anisotropic metamaterials that exhibit negative refraction, IEICE Trans Electron E87-C (2004), 359–370.
7. M. Bayindir, K. Aydin, E. Ozbay, P. Markos, and C.M. Soukoulis, Transmission properties of composite metamaterials in free space, Appl Phys Lett 81 (2002), 120–122.
8. D.R. Smith, J. Gollub, J.J. Mock, W.J. Padilla, and D. Schurig, Calculation and measurement of bianistropy in a split ring resonator metamaterial, J Appl Phys 100 (2006), 024507..
9. J.K. Gansel, M. Wegener, S. Burger, and S. Linden, Gold helix photonic metamaterials: A numerical parameter study, Opt Express 18 (2010), 1059–1069.
10. N. Katsarakis, T. Koschny, M. Kafesaki, E.N. Economou, and C.M. Soukoulis, Electric coupling to the magnetic resonance of split ring resonators, Appl Phys Lett 84 (2004), 2943–2945.
11. J.S. Derov, B.W. Turchinetz, E.E. Crisman, A.J. Drehman, and R. Wing, Negative index metamaterial for selective angular separation of microwaves by polarization, IEEE Antennas Propag Soc Int Symp 4 (2004), 3753–3756.
12. J.S. Derov, B.W. Turchinetz, E.E. Crisman, A.J. Drehman, and S.R. Best, Measured polarization response of negative index metamaterial, In: ICECom 2005: 18th international conference on applied electromagnetics and communications, Dubrovnik, Croatia, 12–14 October 2005, pp. 1–4.
13. J.S. Derov, B.W. Turchinetz, E.E. Crisman, A.J. Drehman, and S.R. Best, The microwave behavior of an anisotropic negative index media, Proceedings of the SPIE optics east, Boston, MA, 12 November 2005.
14. D. Shreiber, M. Gupta, and R. Cravey, Comparative study of 1-D and 2-D metamaterial lens for microwave nondestructive evaluation of dielectric materials, Sens Actuators A 165 (2011), 256–260.
15. D. Shreiber, M. Gupta, and R. Cravey, Microwave nondestructive evaluation of dielectric materials with a metamaterial lens, Sens Actuators A 144 (2008), 48–55.
16. J.B. Pendry, A.J. Holden, J.W. Steward, and I. Youngs, Extremely low frequency plasmons in metallic mesostructures, Phys Rev Lett 76 (1996), 4773–4776.

AN EQUIVALENT CIRCUIT MODEL FOR A MICROSTRIP LINE WITH AN ASYMMETRIC SPIRAL-SHAPED DEFECTED GROUND STRUCTURE

Duk-Jae Woo,[1] Taek-Kyung Lee,[2] and Jae-Wook Lee[2]
[1] Institute of New Media and Communications, Seoul National University, San 56-1, Shillim-dong, Kwanak-Ku, Seoul 151-742, Korea
[2] School of Electronics, Telecommunication, and Computer Engineering, Korea Aerospace University, 76 Hanggongdaehang-ro, Deogyang-gu, Goyang-si, Gyeonggi-do 412-791, South Korea; Corresponding author: tklee@kau.ac.kr

Received 11 September 2013

ABSTRACT: *For a microstrip line with an asymmetric spiral-shaped defected ground structure (DGS), an equivalent circuit model is presented. From the lumped-element circuit model describing the asymmetric properties in circuit elements as well as in their magnetic coupling to the host line, the two rejection frequencies are derived. The equivalent circuit model provides physical insight into the dual-frequency operation of the asymmetric spiral-shaped DGS.* © 2014 Wiley Periodicals, Inc. Microwave Opt Technol Lett 56:1222–1224, 2014; View this article online at wileyonlinelibrary.com. DOI 10.1002/mop.28308

Key words: *asymmetric spiral-DGS; dual-frequency operation; equivalent circuit model*

1. INTRODUCTION

A spiral-shaped defect on the ground plane of a planar transmission line such as a microstrip line or a coplanar waveguide provides a band rejection characteristic at a resonance frequency corresponding to the size of the defect on the ground [1]. The band rejection property of the spiral-shaped defected ground structure (DGS) enables the suppression of undesired harmonics in microwave and millimeter wave circuits [2–5]. To suppress dual frequency bands with conventional symmetric spiral-shaped DGS, DGSs with different defect sizes have to be cascaded. However, the cascaded DGS configuration requires a larger area along the direction of propagation and introduces significant radiation and conductor losses. The dual frequency rejection property from a single asymmetric spiral-shaped DGS has previously been reported by the authors [6]. A microstrip line with an asymmetric spiral-shaped DGS provides two different

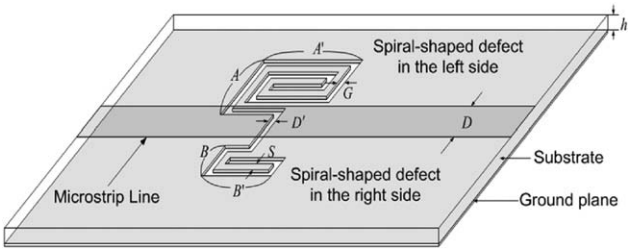

Figure 1 Microstrip line with an asymmetric spiral-shaped DGS

resonance frequencies due to the different defect sizes. Some equivalent circuit models have been presented and these efforts have provided improved design methods and physical insight of the operation principle of the symmetric DGSs [1,7–12].

In this article, an equivalent circuit model is presented to give physical insight into the dual frequency rejection characteristic of the asymmetric spiral-shaped defect on the ground plane of the microstrip line.

2. EQUIVALENT CIRCUIT MODEL

The geometry of the microstrip line with an asymmetric spiral-shaped DGS is shown in Figure 1 where the dimensions of the spiral-shaped defects on the right- and left-hand sides are different [6]. The dimensions are $A = A' = 3.4$ mm, $B = B' = 2.6$ mm, and $D' = S = G = 0.2$ mm, and the structure is on a circuit board GML1000 with a relative dielectric constant of 3.2 and thickness of 1.63 mm. The characteristic impedance of the transmission line is designed to be 50 Ω ($w = 1.2$ mm). The transfer characteristic for the structure in Figure 1 calculated using the electromagnetic full-wave solver (IE3D) is illustrated in Figure 2. It can be seen that a single asymmetric spiral-shaped DGS can provide two different resonance frequencies, that is, 2.56 and 4.22 GHz, due to the different sizes of the defects on the ground plane.

In Figure 1, the electric field concentrates at the narrow etched gap connecting two spiral-shaped defects while the current is confined to the periphery of the etched spiral pattern. Hence the capacitances and inductances of the asymmetric spiral-shaped DGS are determined by the etched gap size and the etched spiral pattern, respectively. The circuit model representing the microstrip line with the asymmetric spiral-shaped DGS is shown in Figure 3(a). From the magnetic wall concept,

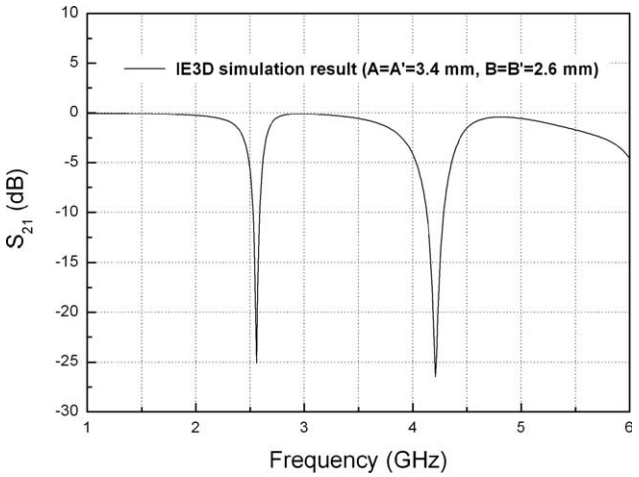

Figure 2 Calculated transfer characteristic of the structure

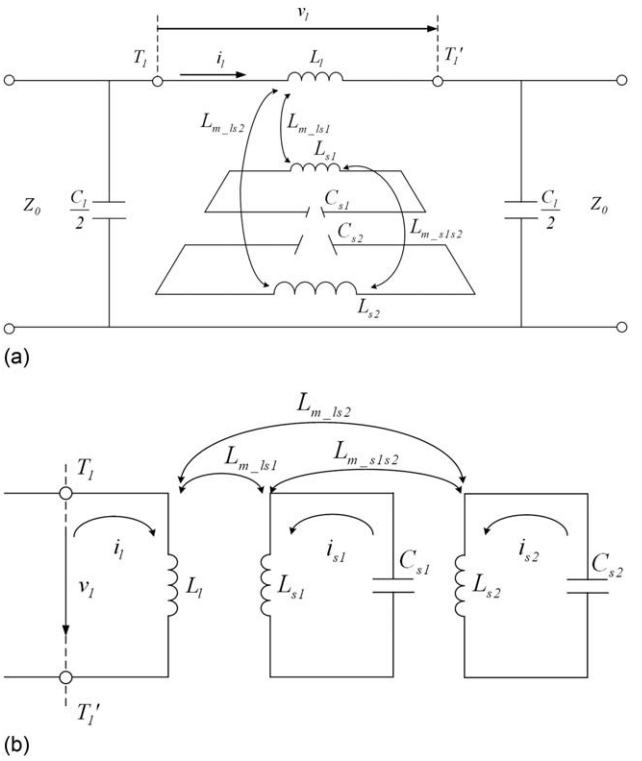

Figure 3 (a) Proposed equivalent lumped element circuit for a microstrip line with an asymmetric spiral-shaped DGS. (b) Equivalent circuit for loop-equation formulation

the unit asymmetric spiral-shaped defect is modeled as two separated LC resonators. These two resonators are magnetically coupled to the host transmission line through mutual inductances L_{m_ls1} and L_{m_ls2}, respectively. Also, L_{m_s1s2} represents the mutual inductance between two resonators. Here, L_1 and C_1 are the per-unit-section inductance and capacitance of the microstrip line.

As the two resonators are coupled with the inductance L_l, the equivalent impedance of the series branch ($Z_{eq\_asy} = v_l/i_l$) between T_1 and T_1' can be obtained from the circuit in Figure 3(b). Three loop equations based on Kirchhoff's law are written to solve the equivalent impedance as follows:

$$j\omega L_l i_l + j\omega L_{m\_ls1} i_{s1} + j\omega L_{m\_ls2} i_{s2} = v_l \tag{1}$$

$$j\omega L_{m\_ls1} i_l + j\omega L_{s1} i_{s1} + \frac{1}{j\omega C_{s1}} i_{s1} + j\omega L_{m\_s1s2} i_{s2} = 0 \tag{2}$$

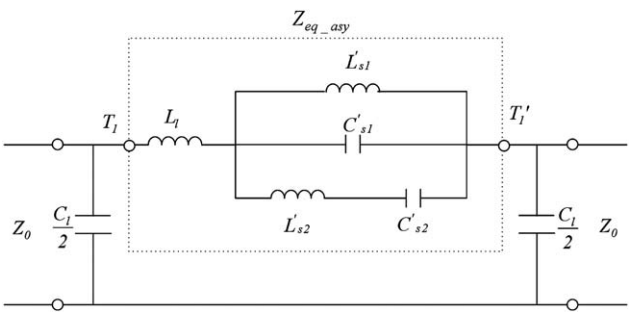

Figure 4 Simplified circuit with the series branch replaced by its equivalent impedance

$$j\omega L_{m\_ls2} i_l + j\omega L_{m\_s1s2} i_{s1} + j\omega L_{s2} i_{s2} + \frac{1}{j\omega C_{s2}} i_{s2} = 0 \tag{3}$$

The equivalent impedance $Z_{\text{eq\_asy}}$ is obtained by solving Eqs. (1)–(3) for i_1 and v_1 as follows:

$$Z_{\text{eq\_asy}} = \frac{v_l}{i_l} = j\omega L_l + \frac{\omega^2 L_{m\_ls1}}{j\omega L_{s1} + \frac{1}{j\omega C_{s1}} + \frac{\omega^2 L_{m\_s1s2}^2}{j\omega L_{s2} + \frac{1}{j\omega C_{s2}}}} i_l + \frac{\omega^2 L_{m\_ls2}^2 \left(\frac{C_{s2}}{C_{s1}} - \omega^2 L_{s1} C_{s2}\right) + 2\omega^4 C_{s2} L_{m\_ls1} L_{m\_ls2} L_{m\_s1s2}}{1 - \omega^2 L_{s2} C_{s2}} \Big/ \left(j\omega L_{s1} + \frac{1}{j\omega C_{s1}} + \frac{\omega^2 L_{m\_s1s2}^2}{j\omega L_{s2} + \frac{1}{j\omega C_{s2}}}\right) i_l \tag{4}$$

From the expression in (4), the series branch impedance between T_1 and T_1' in Figure 3(a) can be replaced by the equivalent circuit as shown in the dotted box in Figure 4. In the equivalent circuit model, the equivalent inductance and capacitances are explicitly $L'_{s1} = C_{s1}A$, $C'_{s1} = L_{s1}/A$, $L'_{s2} = L_{s2}A/B$, $C'_{s2} = C_{s2}B/A$, where

$$A = \omega^2 L_{m\_ls1} + \frac{\omega^2 L_{m\_ls2}^2 \left(\frac{C_{s2}}{C_{s1}} - \omega^2 L_{s1} C_{s2}\right) + 2\omega^4 C_{s2} L_{m\_ls1} L_{m\_ls2} L_{m\_s1s2}}{1 - \omega^2 L_{s2} C_{s2}},$$

$$B = \omega^2 L_{m\_s1s2}^2$$

After some manipulations, the resonant condition of (4) can be written as:

$$\omega^4 (L_{s1} L_{s2} C_{s1} C_{s2} - C_{s1} C_{s2} L_{m\_s1s2}^2) - \omega^2 (L_{s1} C_{s1} + L_{s2} C_{s2}) + 1 = 0. \tag{5}$$

The above biquadratic equation has four solutions, and the two positive real values of the resonance frequencies are

$$\omega_{o1,o2} = \sqrt{\frac{(L_{s1} C_{s1} + L_{s2} C_{s2}) \pm \sqrt{(L_{s1} C_{s1} - L_{s2} C_{s2})^2 + 4 C_{s1} C_{s2} L_{m\_s1s2}^2}}{2(L_{s1} L_{s2} C_{s1} C_{s2} - C_{s1} C_{s2} L_{m\_s1s2}^2)}}. \tag{6}$$

Here, $L_{m\_s1s2} = k_{\text{m}} \sqrt{L_{s1} L_{s2}}$ is the mutual inductance between two resonators and k_{m} is the magnetic coupling coefficient between two resonators.

When k_{m} increases up to 1, the two resonance frequencies in (6) coalesce into a single resonance frequency of $\omega_o = \omega_{o1} = \omega_{o2} = (L_{s1} C_{s1} + L_{s2} C_{s2})^{-1/2}$. For the asymmetric spiral-shaped DGS, however, k_{m} is in practice much lower than 1 so that the asymmetric structure provides two different resonance frequencies.

3. CONCLUSION

The equivalent circuit modeling for an asymmetric spiral-shaped DGS in the microstrip line is presented. Due to the asymmetric structure on the ground plane, the intrinsic circuit has two LC resonators and their resonance frequencies are different. These two resonators are magnetically coupled to each other and also magnetically coupled to the microstrip line. The equivalent circuit model is obtained from the intrinsic resonant circuits and from accounting their couplings, and the two resonance frequencies are derived. The presented equivalent circuit modeling provides physical insights into the behavior of the asymmetric DGS. It also serves as a design guide to the dual band suppression of harmonics for a high frequency circuit.

ACKNOWLEDGMENT

This research was supported by NSL (National Space Lab) program through the National Research Foundation of Korea funded by the Ministry of Science, ICT & Future Planning (No. S10801000159-08A0100-15910).

REFERENCES

1. C.S. Kim, J.S. Lim, S.W. Nam, K.Y. Kang, and D. Ahn, Equivalent circuit modelling of spiral defected ground structure for microstrip line, Electron Lett 38 (2002), 1109–1110.
2. Y.K. Chung, S.S. Jeon, S.H. Kim, D. Ahn, J.I. Choi, and T. Itoh, Multifunctional microstrip transmission lines integrated with defected ground structure for RF front-end application, IEEE Trans Microwave Theory Tech 52 (2004), 1425–1431.
3. J.S. Lim, J.S. Park, Y.T. Lee, D. Ahn, and S.W. Nam, Application of defected ground structure in reducing the size of amplifiers, IEEE Microwave Wireless Compon Lett 12 (2002), 261–263.
4. D.J. Woo, J. W. Lee, and T.K. lee, Multi-band rejection DGS with improved slow-wave effect, In: Proceedings of 38th European Microwave Conference, Amsterdam, The Netherlands, 2008, pp. 1342–1345.
5. Y.T. Lee, J.S. Lim, S.W. Kim, J.C. Lee, S.W. Nam, K.S. Seo, and D. Ahn, Application of CPW based spiral-shaped defected ground structure to the reduction of phase noise in V-band MMIC oscillator, In: IEEE MTT-S International Microwave Symposium Digest 2003, Philadelphia, PA, June 2003, pp. 2253–2256.
6. D.J. Woo and T.K. Lee, Suppression of harmonics on Wilkinson power divider using dual-band rejection by asymmetric DGS, IEEE Trans Microwave Theory Tech 53 (2005), 2139–2144.
7. D. Ahn, J.S. Park, C.S. Kim, J.N. Kin, Y. Qian, and T. Itoh, A design of the low-pass filter using the novel microstrip defected ground structure, IEEE Trans Microwave Theory Tech 49 (2001), 86–93.
8. I.S. Chang and B.S. Lee, Design of defected ground structures for harmonics control for active microstrip antenna, In: Proceedings of IEEE Antennas Propagation Society International Symposium, San Antonio, TX, June 2002, pp. 852–855.
9. C. Caloz, H. Okabe, T. Twai, and T. Itoh, A simple and accurate model for microstrip structures with slotted ground plane, IEEE Microwave Wireless Compon Lett 14 (2004), 133–135.
10. N. Karmakar, S.M. Roy, and I. Balbin, Quasi-static modeling of defected ground structure, IEEE Trans Microwave Theory Tech 54 (2006), 2160–2168.
11. E.O. Hammerstad, Equations for microstrip circuit design, In: Proceedings of European Microwave Conference, Microwave Exhibitor & Publishers, Kent, UK, 1975, pp. 268–272.
12. D.J. Woo, T.K. Lee, and J.W. Lee, Equivalent circuit model for a simple slot-shaped DGS microstrip line, IEEE Microwave Wireless Compon Lett 23 (2013), 447–449.